



INTERNATIONAL ATOMIC ENERGY AGENCY  
UNITED NATIONS EDUCATIONAL, SCIENTIFIC AND CULTURAL ORGANIZATION  
**INTERNATIONAL CENTRE FOR THEORETICAL PHYSICS**  
I.C.T.P., P.O. BOX 586, 34100 TRIESTE, ITALY, CABLE CENTRATOM TRIESTE



UNITED NATIONS INDUSTRIAL DEVELOPMENT ORGANIZATION



**INTERNATIONAL CENTRE FOR SCIENCE AND HIGH TECHNOLOGY**

INTERNATIONAL CENTRE FOR THEORETICAL PHYSICS - 34100 TRIESTE (ITALY) VIA GRIGIANO, 9 (ADRIATICO PALACE) P.O. BOX 586 TELEPHONE 0432/24572 TELEFAX 0432/24573 TELEX 40440 IAPH I

H4.SMR/537-23

**SECOND COLLEGE ON THEORETICAL AND EXPERIMENTAL  
RADIOPROPAGATION PHYSICS**  
(7 January - 1 February 1991)

Co-sponsored by ICTP,  ICSU  
and with the participation of ICS

**ROLE OF IONOSPHERE  
IN MODERN RADIO SYSTEMS**

B. M. Reddy, R. S. Dabas,  
P. K. Banarjee & S. Bhattacharya  
National Physical Laboratory  
New Delhi, India

**ROLE OF IONOSPHERE IN MODERN RADIO SYSTEMS**

Part B

GHz SCINTILLATION STUDIES TO ESTIMATE DEGRADATION  
IN SATELLITE RADIO SYSTEMS

B.M. Reddy, R.S. Dabas, P.K. Banerjee & S. Bhattacharya

National Physical Laboratory,  
New Delhi - 110 012.

JANUARY 1991

Part - B

GHz SCINTILLATION STUDIES TO ESTIMATE DEGRADATION  
IN SATELLITE RADIO SYSTEMS

ABSTRACT

The intervening ionosphere can be a nuisance for satellite-based radio systems. Usually, with increasing frequency the problems become less serious; but they are significant even at 10 GHz. With present day technology, it is not advisable to go beyond 10 GHz, especially in the tropics because of tropospheric phenomena. Thus one has to model the ionospheric effects and optimise system performance. The more important ionospheric effects are phase and amplitude scintillations, group path delay, RF carrier phase advance, Doppler shift, Faraday Rotation and Angular Refraction. A description of these processes is not possible here; but I will show one or two examples to drive home the point that unless we understand, estimate and account for these ionospheric effects, the sophisticated satellite systems will be in jeopardy. Scintillations is one such example and our group at NPL has been working on this problem for 30 years now using many satellites of opportunity. A system designer would require information on signal statistics as well as on morphological aspects of scintillation to be able to assess the problems and to determine the proper fade margin for the links.

Ionospheric scintillation activity is particularly severe around the geomagnetic equator, which passes through the southern part of India. Our observations at 28.6°N latitude shows that the signal at 4/1.5 GHz has faded several times beyond 15 dB peak to peak, and once beyond 24 dB p-p at 4 GHz. Any system engineer would recognise that for a practical digital communication system, a 24 dB fade can severely disrupt communications both digital and analog systems. This report, in addition to describing the morphology of scintillations at 4 GHz, also gives information on signal statistics such as cumulative amplitude distribution, fade duration distribution and signal reliability for different message lengths for some periods of intense scintillations at both C and L Bands. The main objective of this report is to highlight the usefulness of deriving such information from observed data on ionospheric scintillations for radio communication system applications.

1. INTRODUCTION

The ionospheric scintillation phenomenon is one of the most deleterious factors, atleast upto a frequency of 6-7 GHz, in communication systems utilising the earth space path. Such events cause performance degradation to these links when the signal fades below the specified fade margin i.e. below the amount of gain allocated in the power budget of the system to overcome the effect. Not only the links using analog modulation techniques are effected but also the digitally modulated ones experience a disruption in communication, as a drop in signal increases the bit error rate. The increased bit error rate leads to either full or partial loss of a message, depending on the level of degradation. The regions of the earth that are particularly affected by this phenomenon are the subauroral to polar latitudes and a belt surrounding the magnetic equator and the effect is more severe in the latter. In order to assess the problem of degradation caused by scintillations and prepare a systems analysis for a user in the above mentioned regions, two types of data are essential, namely, the signal statistics and the morphology of scintillations [Utlaut, 1974]. The morphology gives us information about the occurrence of scintillations with specific characteristics as a function of latitude, time of the day, season, sunspot and magnetic conditions which in turn helps in forming the scintillation theory. For assessing the effects of ionospheric irregularities on ionospheric communication, what are usually required are suitably averaged values of relevant fading parameters as a function of degree of disturbance existing in the ionosphere. This is the information to which the scintillation theory is capable of contributing [Booker and Tao; 1987]. On the other hand the signal statistics describes the variation of amplitude of scintillations and the rate at which they

occur. The signal statistics along with the morphology aims at presenting the designer of the systems with an evaluation of the problems associated with the propagation path which are likely to be encountered by an operational or a planned satellite link. It also helps to supply the electronic designer with the characteristics of the fading patterns which deteriorate the information flow. Signal statistics in the form of cumulative amplitude distribution, fade rate distribution, message reliability, power spectra and autocorrelation of events corresponding to periods of intense scintillations, gives the system designer pertinent information for implementing schemes to offset the degradation caused by scintillations and to design the specific modulation techniques necessary for the system.

At VHF/UHF frequencies, Whitney and Basu [1977], analysed some scintillation events observed in Huancazo, Peru and Narssarssuaq, Greenland in order to design and evaluate the performance of satellite communication links. Also Mollen et al. [1988], have established empirical relationships between the scintillation depth represented by S4 and peak/fade decibel levels, based on eighteen months of data recorded at Hongkong (22.2° N, 114° E, 10.52 Geomagnetic N (GMN)) using transmissions from INTELSAT (63°) at 4GHz. Since the geomagnetic equator passes through India and most part of it falls within equatorial scintillation beltwidth, communication via the satellites are severely effected by scintillations, and hence it is essential to have a data bank of scintillation morphology and statistics from here. Lakshmi et al. [1988] have reported the signal statistics pertaining to engineering applications of the scintillations at 140 MHz obtained from ATS-6 at Delhi (28.6° N, 77.2° E, 18.9° GMN) along with the morphology of the scintillations at the same frequency for the

Indian zone.

The future earth-space links planned for our country are going to use higher and higher frequencies in the GHz band as well as digital modulation techniques for reliability, flexible traffic handling and increased communication within a given bandwidth. Keeping this in view, we have briefly presented in this paper, the morphology of scintillations at 4 GHz and signal statistics of some of the intense periods of scintillations, based on the telemetry transmissions recorded from the Indian geostationary satellite INSAT 1B (74° E) from July 1984 to January 1990 at Sikandarabad (SKD) satellite earth station (28.48° N, 77.71° E, 24.2° N Mag.lat.) near Delhi. In addition, signal statistics of some of the scintillation events at 1.5 GHz, recorded from the Russian satellite Volna (85° E) at the National Physical Laboratory, New Delhi during March-April 1989 and September-October 1989 have also been analysed. This we hope will help in predicting the limits of future satellite links designed for our country.

## 2. RESULTS AND DISCUSSION

### 2a. Morphology of scintillations

The scintillations at 4 GHz recorded at SKD displayed a remarkable dependence on solar activity. The years 1984 and 1985, corresponding to a low solar activity period, recorded scintillations which never extended beyond 2 dB peak to peak (p-p). The events during these years generally started just after the local sunset and continued beyond midnight. They developed over tens of minutes and the fade rate recorded was of the order of 3-4 fades/min. Analysing the data on a diurnal basis, it was noted that the activity peaked around 2000 to 2100 LT and a second maxima also occurred between 0200 LT and 0300 LT. Seasonal analysis showed that the

maximum percentage occurrence of scintillations was in the summer months (May-June), followed by a moderate activity in the vernal and autumnal equinoxes. Almost no scintillations were recorded in the winter months of November, December and January. Banerjee et al. [1987] have already published a detailed report of the observations made during 1984-1985. As the solar activity decreased further in 1986, no scintillation events were recorded which had a depth beyond 1 dB p-p and hence caused no problem to the satellite communication systems as the fade depth was covered by the usual fade margin of such systems.

The vernal equinox of 1987 again displayed a perceptible increase in scintillation activity and depth. The data analysed for 1987, 1988 and 1989 (details of which are reported in Dabas et al. [1990a]), showed that as the sunspot number increased from 63 in September 1987 to 179.6 in September 1989, the monthly average percentage occurrence of scintillations increased beyond five times (see figure.1). The characteristics and the time of maximum occurrence of scintillations during these years underwent a drastic change. The scintillations during 1987 to 1989 generally occurred in patches one or two hours after the local sunset and continued upto midnight, with peak occurrence around 2000 to 0000 LT. The onset was always very abrupt and developed fully within a few seconds. The fade rate recorded was generally of the order of 14-15 fades/min. The activity became more frequent and intense in the equinoxes with the maximum occurrence percentage recorded during the autumnal equinox (September-October) of 1989. The signal during September-October 1989, more than often faded beyond 15 dB's p-p and once the fade depth exceeded 24 dB p-p. The winter months (November, December and January of 1989-1990) i.e. the winter solstice also recorded an enhanced percentage occurrence of scintillations as compared to that in the low solar activity period.

The activity during the summer months remained same as it was in 1984-1985. Fig.2 gives the seasonal percentage occurrence of scintillations of different levels (namely > 1dB, > 5 dB and > 10 dB) for January 1987 to January 1990. During periods of intense scintillations whenever the fade depth exceeded -8 dB, the antenna tracking system at SKD sounded an alarm, leading to tracking failure and disruption in reception of television picture at S-Band. In general, it was observed that the scintillations were suppressed during geomagnetic disturbances. However, for the cases when the recovery of phase started between midnight to dawn local time sector then the scintillations were found to be enhanced.

Simultaneous observations carried out on a campaign mode at SKD (a low latitude station) and at an equatorial station Chengleppeet (12.67° N, 79.92° E, 5.3° N mag.lat) during September-October 1989, showed that no scintillation events at SKD started without their prior occurrence at Chengleppeet (CHPT) confirming a definite association of the low latitude scintillations with the equatorial ones during the period of observation. The abrupt shooting up of the scintillation depth at the onset itself, at both the stations, indicated that the irregularity causing them was bubble like. Also it was noted that the depth of scintillations at SKD was much higher as compared to that in CHPT. Generally the presence of high electron density at the anomaly crests is associated with the high level of scintillations observed over the earth-space paths crossing them [Aarons et al. 1981]. Though SKD lies far above the day time anomaly crest, but the simultaneous IEC and VHF scintillations observations at different stations by Garg et al. [1983] and Lakha Singh et al. [1990] suggests that during years of high solar activity deep scintillation fadeings at VHF are associated with the postsunset hour shift of the

anomaly crest to low latitudes with a simultaneous electron density depletion at the equatorial stations. This in a way indicates that the high level of scintillations observed at 4 GHz at SKD are associated with the following scenario: As per the fieldline calculations for INSAT-1B ray path geometry [Dabas et al., 1990b] the bubble like irregularities generated at the magnetic equator after the local sunset must rise above 1200 kms for them to map along the field lines to lower latitudes. Since the background electron density at the low latitude station remains high due to occurrence of the postsunset hour anomaly, the plume associated electron density fluctuations are also high in this region and hence the deeper scintillation fadings observed at SKD as compared to that at CHPT. This reasoning has also been found to be true for the observations made at the same frequency by Fang and Liu [1983] at Hongkong.

## 2b. Signal Statistics

### (i) Cumulative amplitude distribution function

Engineers designing the earth-space links must determine the fade margin necessary to overcome the degradation caused by scintillations, under various conditions of the ionosphere and for a particular electronic configuration. The percentage of time that the signal fades below different decibel levels as a function of local time, latitude, season, solar activity and magnetic activity is required for the complete evaluation of the expected performance of the proposed system. The cumulative amplitude distribution function (cdf), a first order statistics, is useful in defining the fade margin requirements for communication systems as it expresses the probability that the signal level will equal or exceed a given decibel level. Whitney et al. [1972], developed a method of representing different cdf's for different

scintillation depths (the scintillation depth have been represented by him as scintillation index SI [Whitney, 1969]), which can be used for practical systems of satellite communication and navigation in the VHF and UHF ranges.

The basic procedure for obtaining a cdf from the raw data corresponding to a certain depth of scintillation is to digitize the data first. Then by applying the criteria of stationarity, a particular segment of the data is finally chosen for estimating the cdf corresponding to it. The S4 index [Briggs and Parkins, 1963], dependent on the rms value of the power of the signal and hence also a measure of depth of scintillation, has been calculated for every one minute interval of the scintillation event under consideration. Ideally the condition for stationarity implies that the s4 index should be time invariant, which is practically not possible. Therefore we have chosen a criteria for stationarity according to which the standard deviation of the s4 index should always be less than twenty percent through out the duration of the segment [Quinn, 1980]. The date and duration of some of the events that have been analysed are given in Table-1 for both L-Band and C-Band.

TABLE-1

Frequency	Date	Duration (LT)	Number of one min. intervals
4 GHz	5th Oct. 1989	2054 - 2148	54
	6th Oct. 1989	2030 - 2200	90
	14th Oct. 1989	2218 - 2255	32
1.5 GHz	14th Apr. 1989	2152 - 2319	87
	30th Sep. 1989	2107 - 2237	30

Depending on the condition of stationarity, the sample lengths which have been used for our analysis range from a minimum of 3 minutes to a maximum of 7 minutes. Two computer plotted scintillation samples at 4 GHz, one strong and one weak, with  $s_4$  indices 1.2 and 0.31 are shown in figure.3a and figure.3b respectively. Infact the sample corresponding to  $s_4$ : 1.2, corresponds to the maximum fade depth recorded so far at this frequency. The respective cdf's are shown in figure.3c. It can be seen from the cdf's that there is a strong correlation between the depth of fade and peak enhancements with increasing  $s_4$  index. The level of scintillations which are of particular interest to a system engineer and can be read from the cdf are the peak enhancement, maximum fade, 5% peak and 95% fade. These statistical signal levels in decibel magnitude corresponding to the cdf's in figure.3c. are given in Table-II. Similarly two samples of scintillations at L-Band with scintillation indices of 0.85 and 0.34 are shown in figure.4a and 4b respectively. The cdf's of these samples are presented in figure 4c and the corresponding decibel levels given in Table-II.

TABLE II

Frequency (GHz)	$s_4$ Index	Peak Enhancement (dB)	Maximum Fade (dB)	Five Percent Peak (dB)	Ninetyfive Percent Fade (dB)
4.0	1.2	12.0	-12.6	8.0	-8.2
	0.31	3.8	-5.4	2.0	-2.6
1.5	0.85	9.0	-11.8	6.2	-8.4
	0.34	3.0	-4.4	2.2	-2.6

According to Rufenach [1975] scintillation model, the irregularities in the ionosphere act as a screen to the incident wave front and changes its

phase when it passes through the layer. After emerging from the ionosphere, phase disturbed waves turn gradually to amplitude modulated waves while propagating along their paths due to the diffraction effect and finally the wave at a point sufficiently far from the ionosphere can be regarded as the sum of the unperturbed field i.e. the coherent component and the perturbed field, the incoherent component. Based on this discussion, the theoretical cumulative probability distribution of the ionospheric scintillations results in the Nakagami-Rice distribution [Karasawa et al., 1985]. Various researchers, on the otherhand have shown that, the cumulative distribution function of the ionospheric scintillations follow the Nakagami-m distribution, where  $m=1/S_4^2$  [Whitney, 1972; Crane, 1977; Yeh and Liu, 1982; Mollen et al., 1988]. Since the Nakagami-Rice distribution is similar to the Nakagami-m distribution for all values of  $m>1$ , discussion on the comparative merits of the two is of little significance from the practical point of view. Comparison between the observed cdf and theoretical Nakagami-m and Log-Normal distributions were evaluated for our data. It is seen that the Log-Normal distribution is a better fit for the scintillation events with  $s_4$  values less than 0.5 i.e. for weak scintillation cases, whereas for strong ones, the Nakagami-m distribution clearly appears to be the best fit. This is true for both L-Band and C-Band as can be seen from figure.3c and figure.4c respectively. Therefore our observations also establish that for all practical purpose the Nakagami-m distribution for various values of  $s_4$  can be used by engineers for determining the fade margin of a system.

The scintillation recordings obtained at Sikandarabad at 4 GHz and 1.5 GHz have been grouped into three categories according to  $s_4$  values. The first category comprises of several recordings of one minute intervals

with the  $s_4$  index in the range of 0.3-0.59, 0.6-0.79 and 0.80-1.0. A minimum of fifteen to twenty recordings are considered in each of the categories for obtaining a model amplitude distribution curve for that range of  $s_4$ . Cumulative amplitude distribution function was obtained individually for all the one minute recordings similar to that shown in figure.3 and figure.4. A model cdf was obtained for each of the categories by determining the median of all the distributions in that category. Figure.5 shows the median model distributions for the three categories mentioned above.

#### (ii) Fade duration distribution

Information on distribution of fades of different durations or the fade rate distribution for various levels of fade margin is needed in order to fully characterise the effects of scintillations on the communication channels, specifically for choosing the coding or diversity techniques to combat fading. For high speed digital transmission, problems are the statistics of duration of fades below a particular level. If the duration of fades is longer compared to the information pulse length (spacing between successive pulses in digital transmission) and the fade depth to a value below system sensitivity, information bits could be lost. The fade rate distribution can either be produced by the level crossing techniques or by Fourier techniques which gives a power spectra and time correlation function. In this paper we have firstly obtained the fade duration distribution by making use of the level crossing method [Whitney and Basu, 1977]. The level crossing data gives measurement of distribution of the fades and enhancements at various levels with respect to the median level. The duration of separation of the fades are counted at each level for every 1 dB change. Similarly the separation intervals can be counted

for all the levels in order to have a signal enhancement duration distribution.

Figure.6a and figure.6b show the distribution of fades below several levels for both C-band and L band corresponding to the scintillation samples shown in figure.3a and figure.4a respectively. Intervals shorter than 0.5 seconds at 4 GHz and 0.05 seconds at 1.5 GHz could not be resolved as the C Band data was digitised manually from a strip chart recorder run at a speed of 12 cm/min where as the L Band data was recorded via a microprocessor based data acquisition system at the rate of twenty data points every one second. It can be seen from figure.3 that at 4 GHz when the fade margin is -2 dB, the cumulative number of fades corresponding to a duration of 5 seconds or less is 16. Similarly at 1.5 GHz the number of fades with durations 5 seconds or less at -2 db fade level are 68. This confirms the fact that even at frequencies as high as in the GHz range the fade rate has decreased with the increase in frequency. According to our observations the fade rate has decreased two to four times for all the fade levels when the frequency has increased from 1.5 GHz to 4 GHz.

#### (iii) Message reliability

The loss of information due to ionospheric scintillations is also dependent on the message length. A perfect message is received only during those intervals when the signal level is greater than the fade margin. Figure.7a and figure.7b show plots of message reliability at C and L Bands for the scintillation events shown in figure.3a and figure.4a respectively. This gives an estimate of the increase in margin which is required over the value specified by the cdf to obtain a given probability of receiving perfect messages. Message reliability was estimated by determining the number of time intervals or windows that completely fit

within the signal enhancements or increases above certain specified calibration level compared with the total possible number in the entire sample segment under consideration [Whitney and Basu; 1977]. As the time interval of the message length approaches zero, the message reliability approaches the percentile given by the cdf at that fade level. This means that the cdf gives the maximum value of message reliability for a particular fade level. It can be seen from fig.7 that for a given fade margin the message reliability decreases as the message length increases. For C Band at -8 dB level, seventy five percent of the messages are perfectly received if the message length is of ten seconds, whereas for L Band fifty percent of the messages are perfectly received for the same message length. If the fading rate is so fast that the separation time intervals are lesser than the message length, then no messages will be received without error. Also we observe from figure.7 that the message reliability curves fall off more rapidly as the fading rate increases from 5 fades per minute in C Band to 14 fades per minute in L Band.

(iv) Power spectrum and autocorrelation analysis

The power spectrum of the scintillation events contain information about the spectral content of the irregularities which cause scintillations when the radio wave passes through it. It generally consist of a low frequency flat portion and a high frequency roll off. The break frequency between the two parts corresponds to the fresnel frequency. The fresnel frequency is defined [Ott; 1977] as approximately equal to the velocity of the medium transverse to the radio ray path divided by the radius of the first fresnel zone, and is represented as

$$f_c = v / \lambda \left( \frac{2z}{\lambda} \right)^{1/2} \quad (1)$$

where v is the mean drift velocity of the scintillating medium transverse

to the radio path,  $\lambda$  is the wavelength and z is the mean height of the medium. Depending on the geometry between the radio ray path and the motion of the irregularities, oscillations may appear in the spectrum as it decays. The study of power spectrum is valuable to the physicist who wishes to identify parameters like scale sizes, elongations and drift velocities of the irregularities which will help to determine the physical origin of the scintillations. Irregularities of the size corresponding to the fresnel scale contribute most to the amplitude scintillations observed on the ground for weak scintillations. Fresnel zone size also determines the correlation distance of the signal received on the ground. The slope of the rolloff portion of the spectrum is important because it is related to the dissipation rate of the ionospheric irregularities causing the scintillations [Mollen et.al.;1988]. If the amplitude spectra fall off with constant slope, estimates of the spectral power in the higher frequency components (short time periods) may be obtained [Ott, 1977]. These higher frequency estimates are extremely applicable to high-data rate systems where the interest is in determining if scintillations occur on a macro-to-nanosecond time scale. Whitney [1976] has observed a cutoff frequency for power spectra for intense scintillations at 137 and 360 MHz. He defines a bandwidth in terms of this cutoff frequency for use in coding techniques. Also the mean duration of fades is proportional to the average fade rate and thus to the width of the fading power spectrum (the width between the fresnel frequency and the frequency at which the noise level starts). Communication engineers who realize that a 24 dB fade completely blanks out a digital transmission (such as the four phase PSK/TDMA) as the increased fade depth causes intense phase scattering/jitter leading to pulse broadening. Therefore the interpulse spacing is disturbed resulting in a message being transferred at an unacceptably high bit error rate.



When the scintillation strength increases, the signal is presumed to have undergone multiple scattering or refractive scattering. Broadening of the spectrum is observed because the multiple scattering, that comes into play decorrelates the scintillating signal [Yeh,1975; Basu and Basu,1981; Rino and Owen,1981] and as such the association of the break frequency with the fresnel frequency is not very clear. The spectral shape correspondingly therefore should not show any sharp break around the expected fresnel frequency. Our results ( see fig.8) show, that the width of the spectrum has increased with the increase in scintillation strength at L-Band, whereas it is not the same in C-Band. The dashed and the solid vertical lines in figure.8 correspond to the theoretical fresnel frequency and the starting of the noise level of the spectrum. The slopes of the spectrums so far calculated show a variation between -2.5 and -5.5. Table III specifically gives the values of the slope corresponding to the power spectrums in figure.8.

The autocorrelation analysis of the digitized scintillation data establishes a correlation interval  $t$ , which is defined as the time lag for which the level of correlation of the signal decreases to fifty percent of its maximum value. The autocorrelation analysis is another way of characterising the scintillation fading and is an effective means of acheiving time diversity improvements. For scintillations the correlation interval of the signal is approximately related to the Fresnel zone by

$$t = (\lambda z)^{1/2} / v \quad (2)$$

The correlation interval multiplied by the velocity transverse to the ray path will always give the decorrelation distance on the ground. This is same as the Fresnel scale size in case of weak /diffractive scattering. Whereas in the strong cases the actual scalesize of the irregularities

cannot be determined from autocorrelation analysis. However the ground decorrelation distance obtained from the correlation interval in both the cases can be used for antenna diversity in critical applications. Also by taking the inverse of the fifty percent correlation time the fading rate can be estimated. The correlation interval, in general, decreases faster in case of strong scintillations. Fig.9 shows the lag time vs. autocorrelation function for the events in fig.3 and fig.4. For all the events analysed, the fifty percent decorrelation time is ranging from 0.5 seconds to 2 seconds in C Band and from 0.5 to 1.0 seconds in L Band respectively. Table III also gives the ground correlation distance corresponding to the autocorrelation intervals obtained from figure.9a and figure.9b by taking a median drift velocity of 90 m/s transverse to the ray path [Dabas et al.,1990b]. We find that as expected [Umeki et al.,1977] the broadening of the spectra is closely related to the correlation interval. It is seen that, smaller the fifty percent decorrelation time is, more the spectrum has broadend.

A comparison of fade rates obtained from the three methods, namely the mean crossing method, power spectrum analysis and the autocorrelation method is given in Table IV. All these values pertain to the scintillation patches shown in figure.3 and figure.4.

TABLE III

Frequency (GHz)	s4 index	slope	Fresnel frequency (mHZ)	Theoretical ground decorrelation distance(mtr.)	Fifty percent corr. time(sec)	Observed ground decorr. distance(mtr)
4.0	1.26	-2.60	320.0	83.4	2.00	---
	0.31	-4.50	250.0	67.5	0.58	44.0
1.5	0.85	-3.85	---	---	0.45	---

0.34    -2.40    250.0    98.0    0.48    79.0

TABLE IV

Frequency (GHz)	Average fade rate in Hz		
	Mean level crossing	Power spectrum analysis	1/e correlation time
4.0	0.25	0.48	0.50
1.5	0.26	0.46	0.52

(v) Frequency Dependence

The frequency dependence of the ionospheric scintillations is also of interest to the designer of communication systems. Often data is not available for a specific frequency band that is of interest. Some means of extrapolating fading information from other frequency ranges in a usable form is valuable. The frequency dependence can be determined by relating the ratio of amount of power in the scintillating component to the frequency ratio. Whitney et al. [1972] have shown that the spectral index or the frequency dependence can be related to the Nakagami-m parameter by the relation

$$-2n = \frac{[\log(m_1/m_2)]}{\log(f_1/f_2)} \quad (3)$$

where n is the spectral index and  $m_1$  and  $m_2$  are the Nakagami parameters measured at the two frequencies. Moreover this frequency is valid as long as S4 is constant power law of frequency. A log-log plot of S4 vs f will give us a straight line with a slope equal to n. If n can be evaluated from simultaneous distributions for two frequencies from the same source, then the prediction of the expected distribution at a desired frequency can be made as long as the scintillation index and the nakagami-m

parameter remains a constant power of frequency. Whitney et al. [1972] showed that if the experimental cdf's at two frequencies at two different m values are known then by using eq(3) we can find n. On assuming that n is constant within the frequency range, we can find out the cdf for an inbetween frequency for a given m by using the theoretical distribution which fits the experimental ones for a given region. Since we have not been able to record the two frequencies 4 and 1.5 GHz simultaneously from the same satellite, the frequency law could not be verified for our case. Also if strong scattering is observed i.e. S4 > 0.5, then a constant power law relationship may not hold, and interpolation or extrapolation for a distribution at other frequencies may not be feasible.

4. FUTURE STUDIES

It is suggested that simultaneous observations should be taken at different latitudes, (not only two, as done in our case) starting from the equator and at two different frequencies from the same source, in order to provide useful parameter for global scintillation modelling, which is urgently required for our region. The scintillations at two frequencies are necessary to determine the frequency dependence. The experiment should be planned in such a way so that all the observation stations should be along the same geomagnetic meridian. A receiver should also be installed beyond the anomaly peak, in order to know how far the high intensity scintillation belt shifts to the North during the equinox periods of high solar activity years. To study the longitudinal variation in the occurrence of scintillations, a fourth receiver should be installed at the anomaly peak but separated in longitude with respect to the other stations.

In the present study we have estimated the amplitude and rate

characteristics of intense scintillations at C/L Bands from a large collection of data for about half a solar cycle. The results are in the form of cumulative amplitude distribution function, level crossing tabulations, power spectra and correlation data. The Nakagami-m distribution was found to be the best distribution for describing the percentage of time the signal faded below a level with the Rayleigh distribution as the limiting case, which is in agreement with the spectral index characteristics which indicates that fading of the most intense samples is almost independent of frequency [Whitney and Basu, 1977]. The autocorrelation and the power spectra data defined the fade rates and provided a base for the evaluation of time diversity techniques. Much remains to be done to characterize the intense scintillations that are observed in this region. Multifrequency observations are necessary to determine the frequency dependence and the evaluation of diversity techniques.

Acknowledgement We are extremely grateful to Mr. S. Raizada, scientist, Computer Division, National Physical Laboratory, for guiding us to devise some of the programmes involved in the above work.

#### REFERENCES

- Banerjee, P K, M Mohan, S Bhattacharya, B M Reddy and J Singh; SHF scintillation studies using transmissions from the geostationary satellite INSAT-1B; Conf. Proc. IEE, April 1987, U K.
- Basu, S and S Basu; Equatorial scintillations - A review; J Atmos Terr Phys., 43, 473, 1981.
- Booker, Henry. G., Jing-Wei Tao; A scintillation theory of the fading of HF waves returned from the F-region: receiver near transmitter; J. Atmos. Terr. Phys.; 49, 9, 915-938, 1987.
- Briggs, B H and I A Parkin; On the variation of radio star and satellite scintillations with zenith angle; J Atmos. Terr. Phys., 25, 339-336, 1963.
- Crane, R K; Ionospheric scintillations; Proc. IEEE, 65, 2, 180, 1977.
- Dabas, R S, P K Banerjee, Sumana Bhattacharya, B M Reddy and J Singh; GHz scintillation observations at 22.0 N magnetic latitude in the Indian zone; Radio Science, 1990a (in press).
- Dabas, R S, P K Banerjee, Sumana Bhattacharya, B M Reddy and J Singh; Equatorial plasma bubble dynamics; J. Atmos. Terr. Phys., 1990b [communicated].
- Fang D J and C H Liu; A morphological study of GHz scintillations in the Asian region; Radio Sci., 18, 2, 241-252, 1983.
- Garg, S C, Y V Somayajulu, L Singh, T R Tyagi; Evidence of the development and decay of a post sunset equatorial anomaly at low latitudes; Supplement\* to Proc. of International Symposium on 'Beacon satellite studies of the earths environment, Delhi, Feb 7-11, 359-366, 1983.
- Karasawa Y, K Yasukawa and M Yamada; Ionospheric scintillation measurements at 1.5 GHz in midlatitude region; Radio Sci., 20, 3, 643-

651, 1985.

Lakshmi, D R, R S Dabas, L Singh; Studies on ionospheric scintillations for radio system applications, N P L report no.: NPL-88-c.5-006, February 1988.

Mollen, T A, C H Liu, D J Fang; A study of C-band equatorial scintillations in the Asian sector; Radio Science, Vol.23, no.3, 337-345, 1988.

Ott, R H; Observed temporal amplitude and phase spectra from ATS-6 radio beacon experiment at 40, 140 and 360 MHz; Radio Sci., 12, 2, 319-325, 1977.

Quinn, Stanley B Jr.; Studies of Transionospheric scintillation using orbiting satellite data; Deptt. of Electrical Engineering Univ. of Illinois at Urbana Champaign, Urbana, Illinois 61801, AFGL-TR-80-0092, Scientific Report, No.2; AFGL, Air Force Systems Command, U S Air Force, Hanscom AFB, Massachusetts 01731, April 1980.

Rino C L and J Owen, On the temporal coherence loss of strongly scintillating signals; Radio Sci., 16, 31-33, 1981.

Rufenach, C L; Ionospheric scintillation by random phase screen approach, Radio Sci., 10, 155-161, 1975.

Singh Lakha; J K Gupta, P N Vijay Kumar and T R Tyagi; Morphological study of postsunset secondary maximum in ionospheric electron content and its correlation with Faraday polarization fluctuations and VHF amplitude scintillations at Delhi; Proc. Beacon Satellite Symp., Tucuman, Argentina, 1990.

Umeki, R, C H Liu and K C Yeh, Multifrequency spectra of ionospheric amplitude scintillations, J Geophys. Res., 82, 2752-2760, 1977.

Utlaut, William F. Ionospheric scintillations a potential limitation to

satellite communications - important unknown scintillation factors; AIAA 12th Aerospace Science Meeting; Washington D C, Jan 30 - Feb 1, 1974.

Whitney, H E, C Malik and J Aarons, A proposed index for measuring ionospheric scintillations; Planet. Space Sci., 17, 1069-1073, 1969.

Whitney H E, J Aarons, R S Allen and D R Seeman; Estimation of Cumulative amplitude probability distribution function of ionospheric scintillations; Radio Sci., vol.7, no.12, 1095-1104, December 1972.

Whitney H E and Basu S; The effect of ionospheric scintillation on VHF/UHF satellite communications, Radio sci., vol.12, no.1, pg.123-133, Jan-Feb 1977.

Yeh, 1975

Yeh, K C and C H Liu; Radio wave scintillations in the ionosphere, Proc. IEEE, 70, 4, 324-360, 1982.

Figure Captions

Fig.1. Variation of monthly mean nighttime scintillations with the monthly mean sunspot number from January 1987 to December 1989.

Fig.2. Percentage occurrence of nighttime scintillations (peak to peak deviations >1 dB, >5 dB and >10 dB) for the period January 1987 to January 1990.

Fig.3. Computer plotted scintillation samples in C-Band: (a) 5<sup>th</sup> October 1989;  $s_4=1.2$  and (b) 14<sup>th</sup> April 1989;  $s_4=0.31$ . The corresponding cumulative distribution functions are shown in (c).

Fig.4. Computer plotted scintillation samples in L-Band: (a) 30<sup>th</sup> September,  $s_4=0.85$ ; (b) 30<sup>th</sup> September 1989,  $s_4=0.34$ . The corresponding cumulative distribution function are shown in (c).

Fig.5. Cumulative fade duration distribution for three  $s_4$  groups as mentioned within the graph (for L and C bands both)

Fig.6. Fade duration distribution for different fade levels corresponding to the two scintillation samples shown in fig.3 and fig.4.

Fig.7. Graph for percentage of messages perfectly received as a function of message length and fade margin for data corresponding to fig.3 and fig.4.

Fig.8. Power spectrum curves for the scintillation samples at 4 GHz and 1.5 GHz as shown in fig.3 and fig.4 respectively. The dashed vertical lines corresponds to the theoretical fresnel frequency and the solid lines to the starting of the noise floor.

Fig.9. Autocorrelation curves of the samples shown in fig.3 and fig.4.

23  
*to noise ratio*

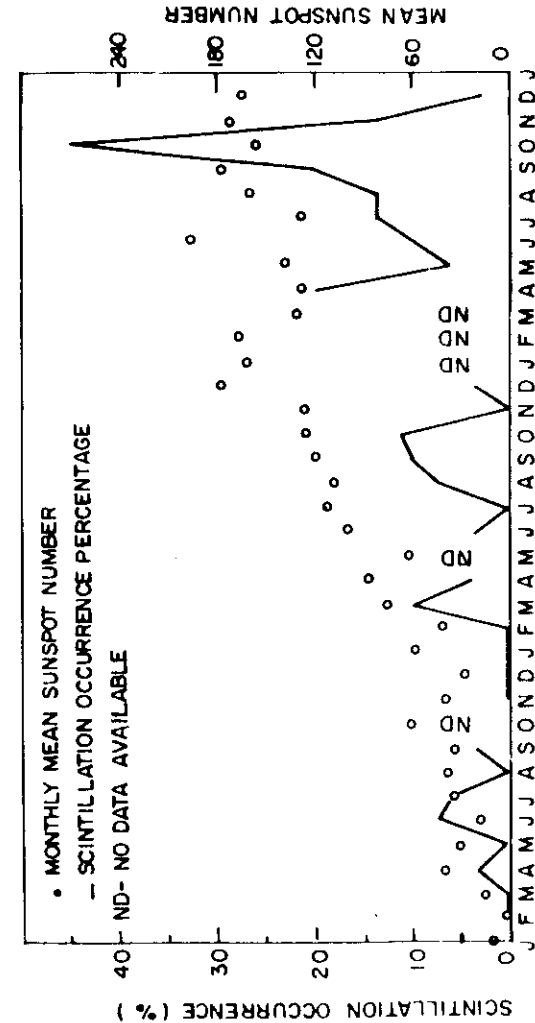


Fig. 1

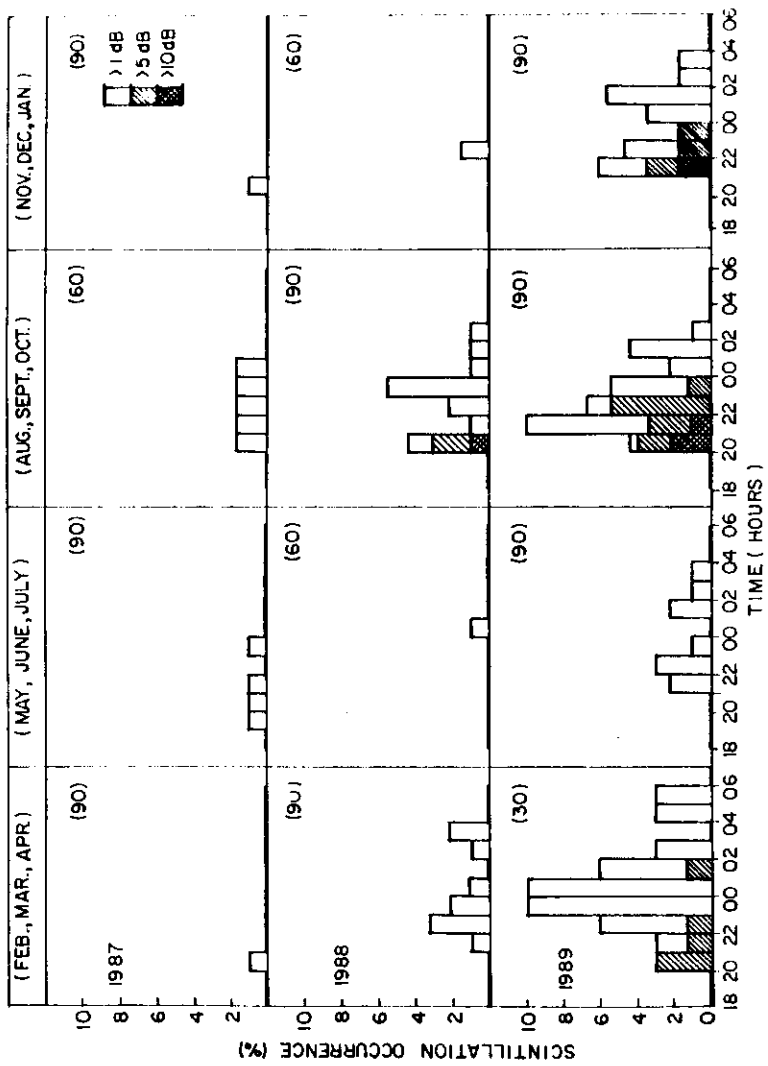


FIG. 2

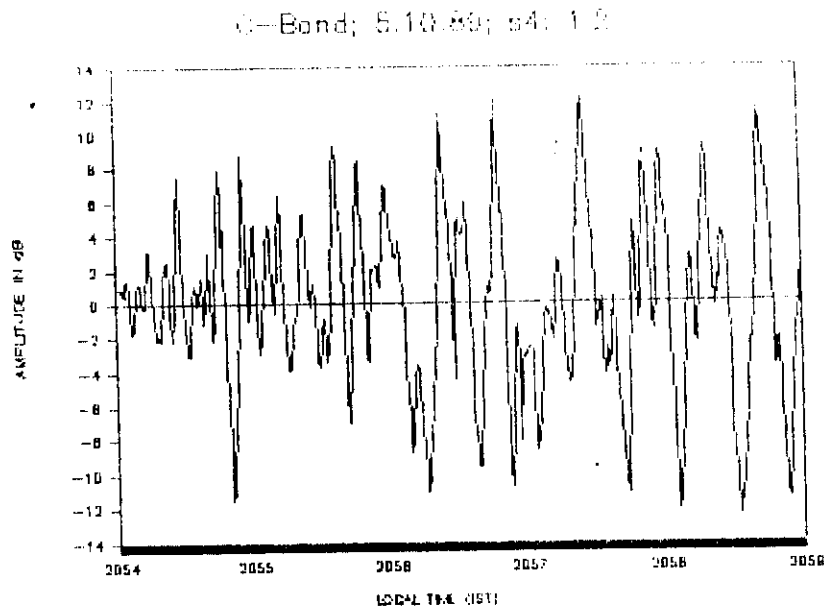


FIGURE 3a

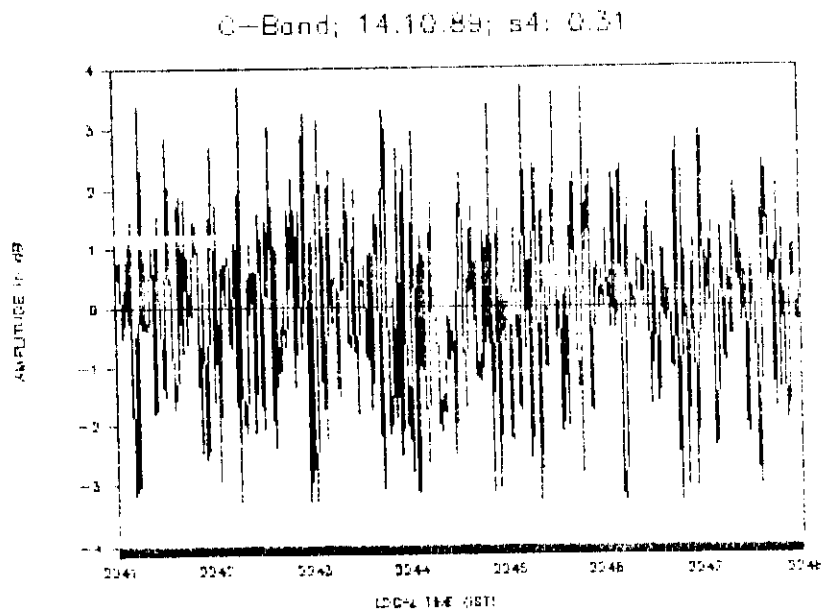


FIGURE 3b

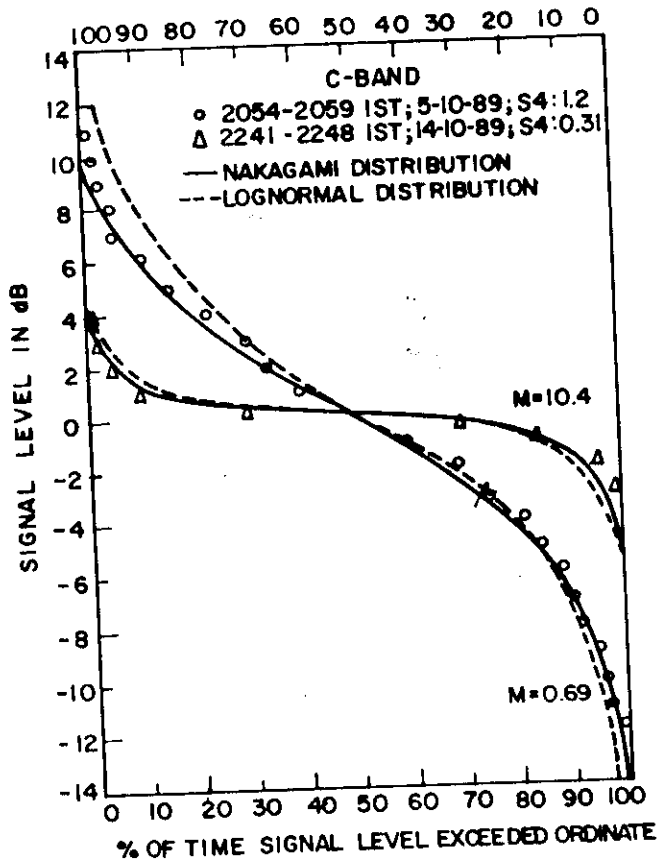


FIGURE 3C

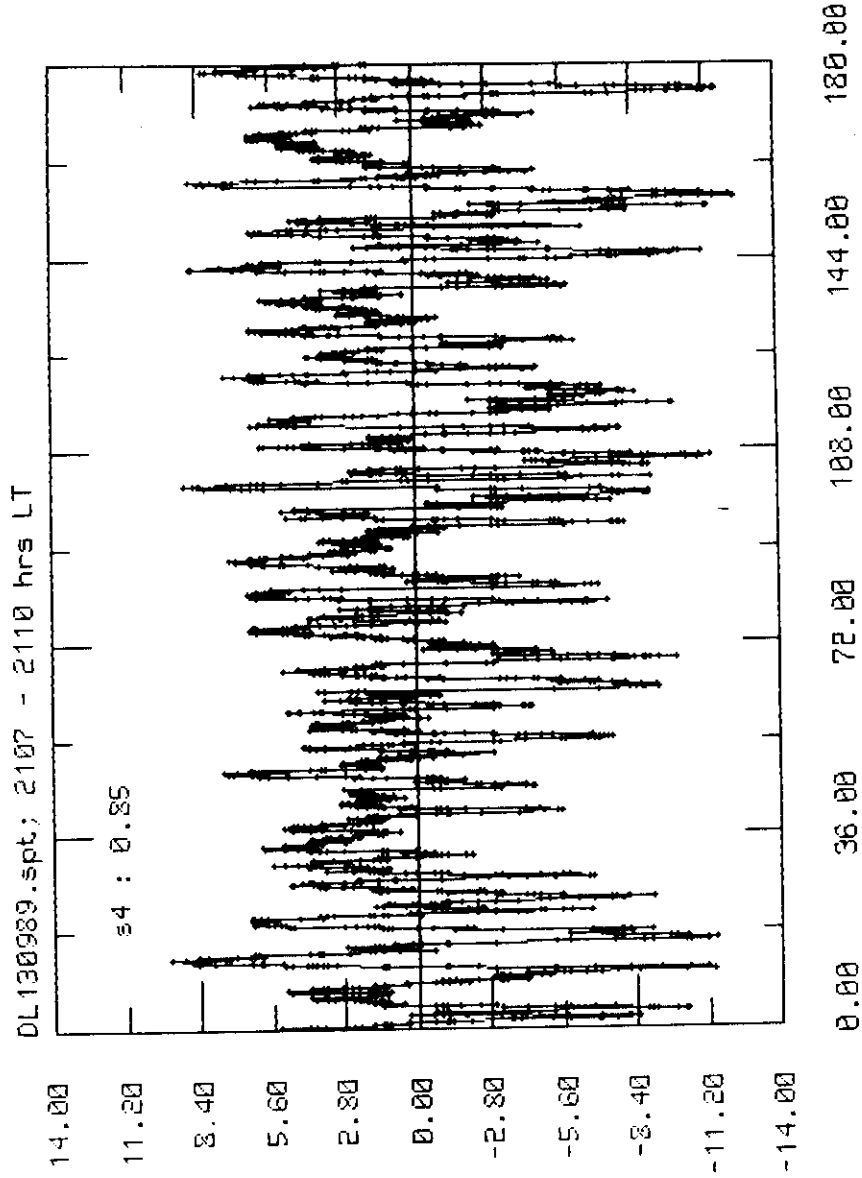
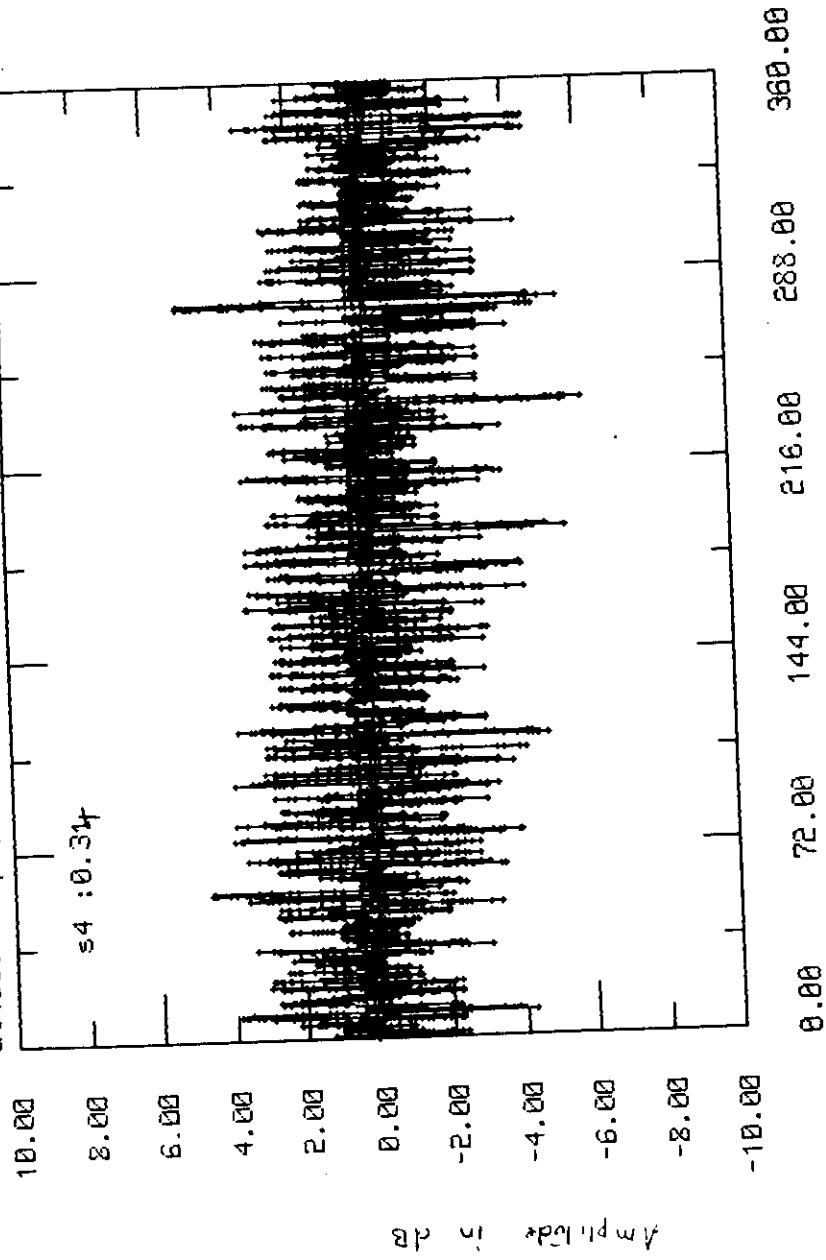


FIGURE 4A

d1130989.spt; 2130 - 2136 hrs



time in seconds

FIGURE : 4b.

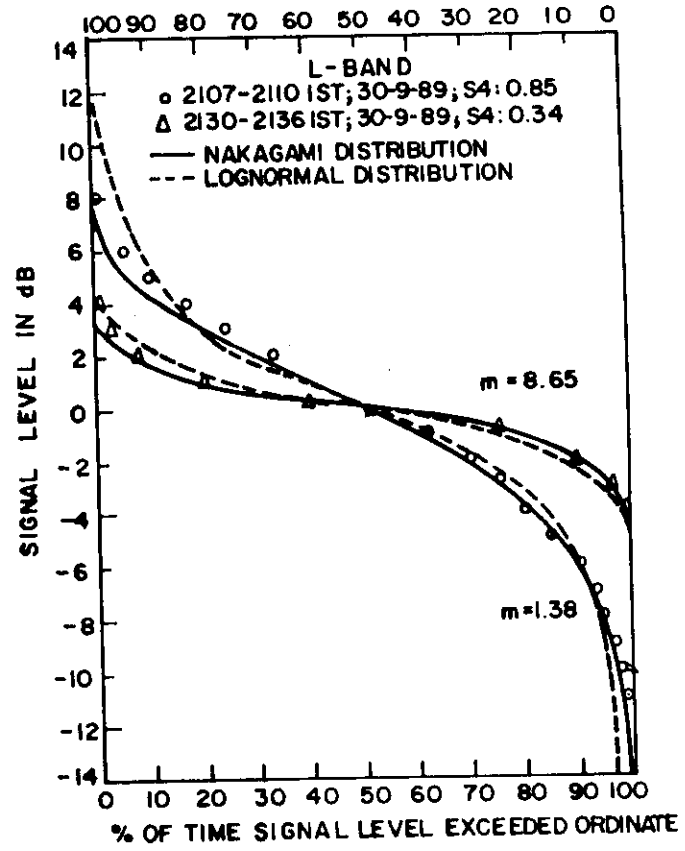


FIGURE : 4c



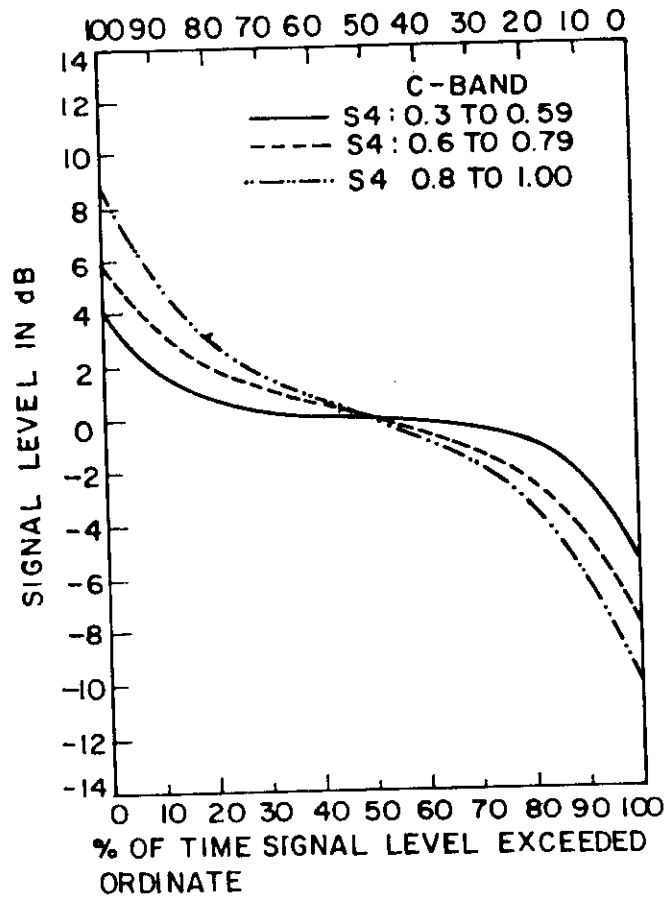


FIGURE 5a

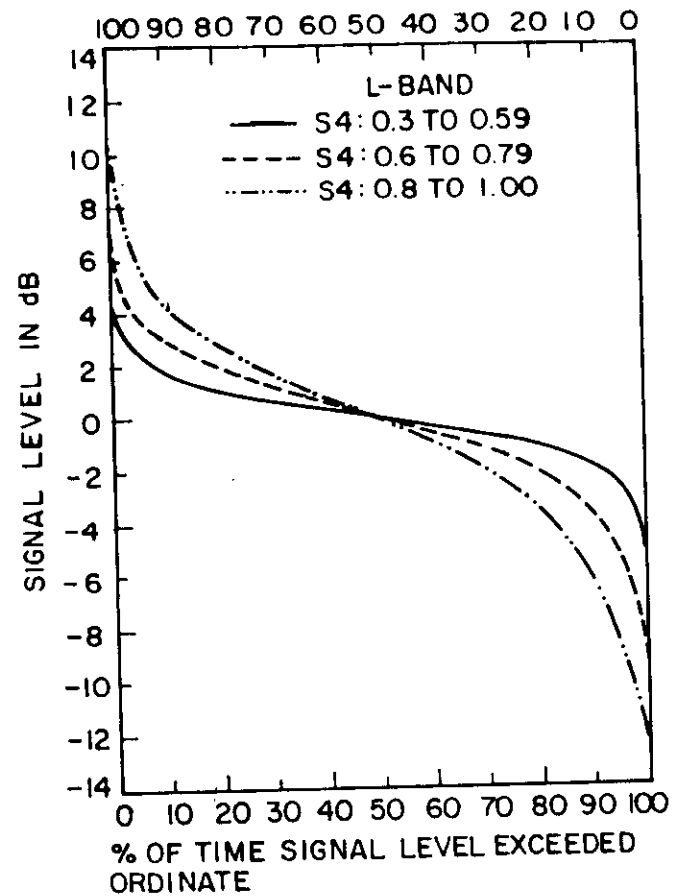


FIGURE 5b

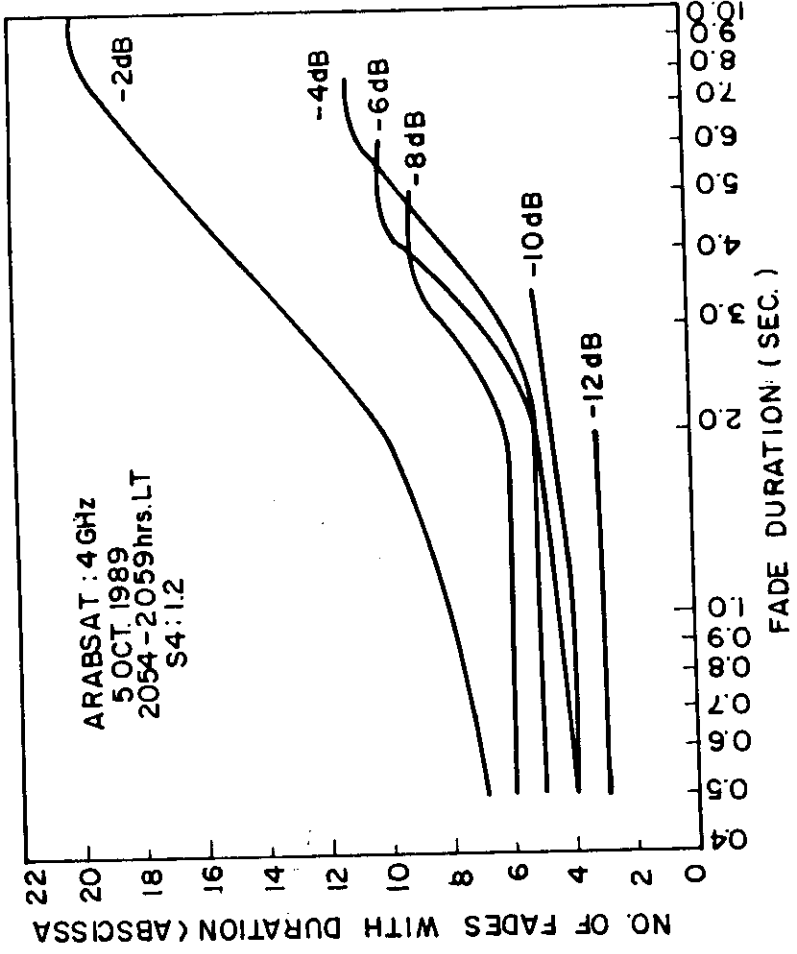


Figure 6a

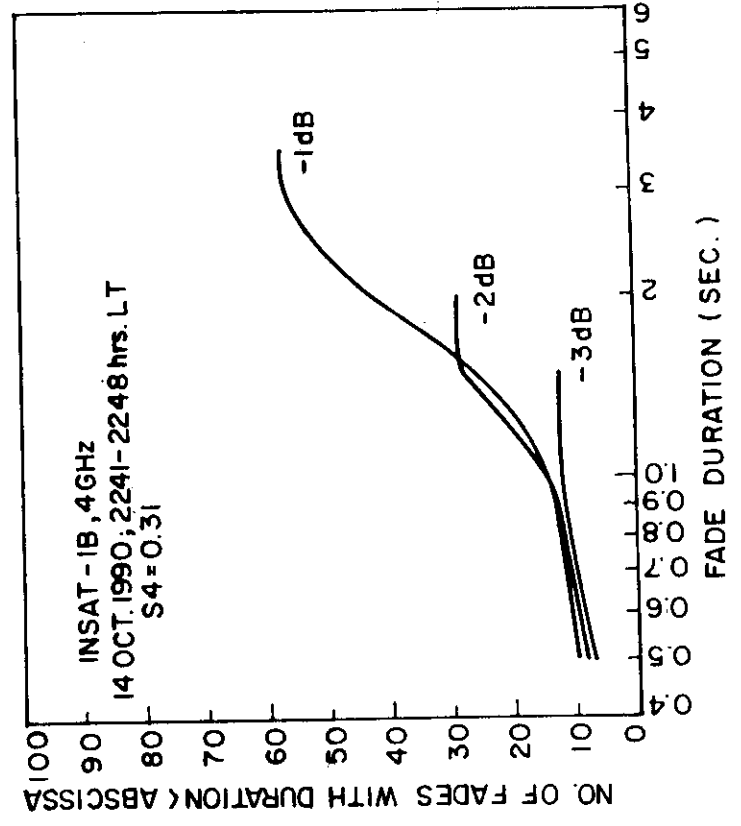


Figure 6b

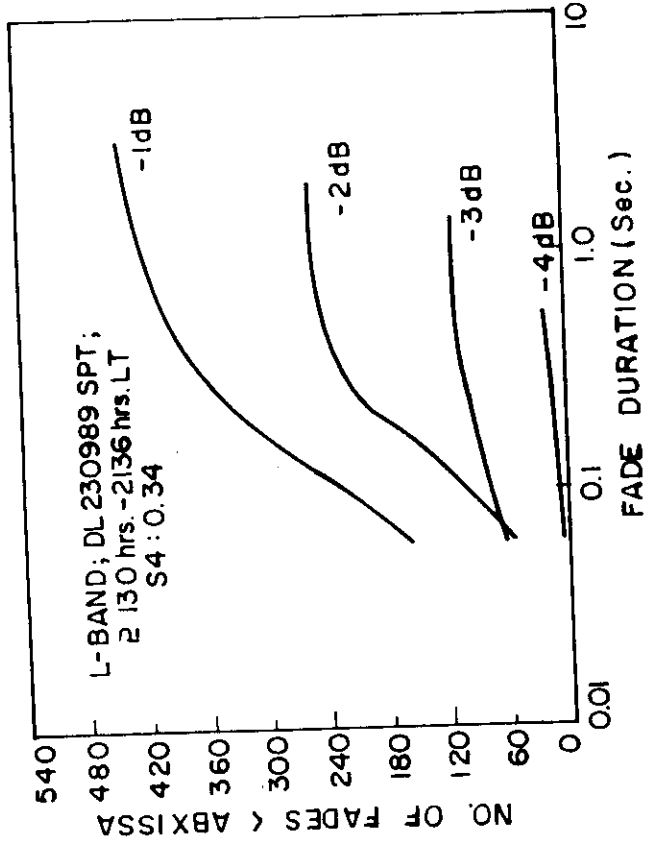


FIGURE 6c

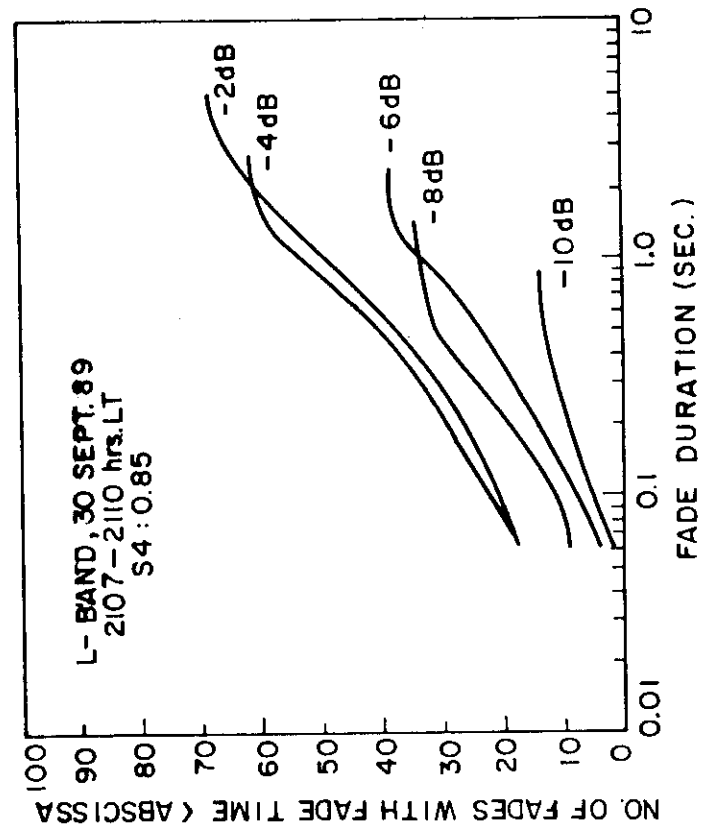


FIGURE 6d

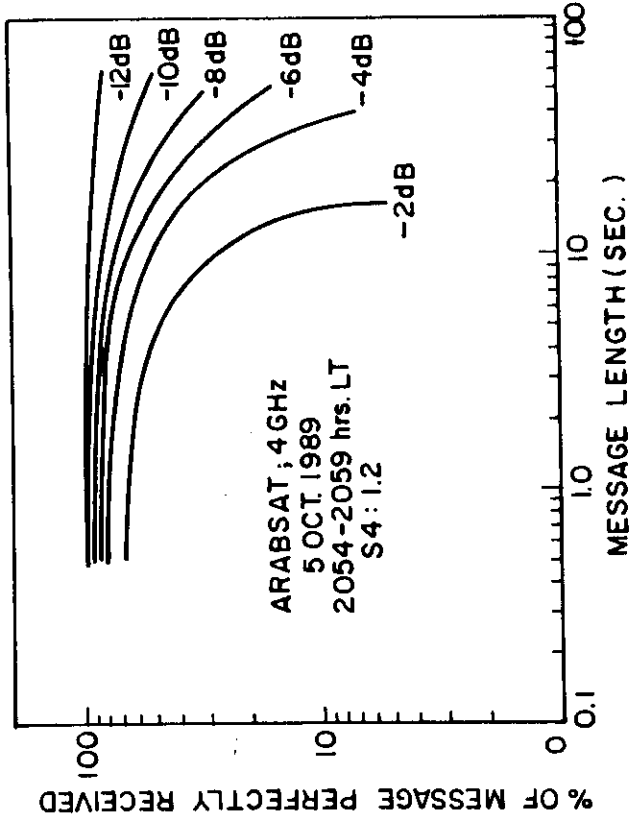


FIGURE 7a

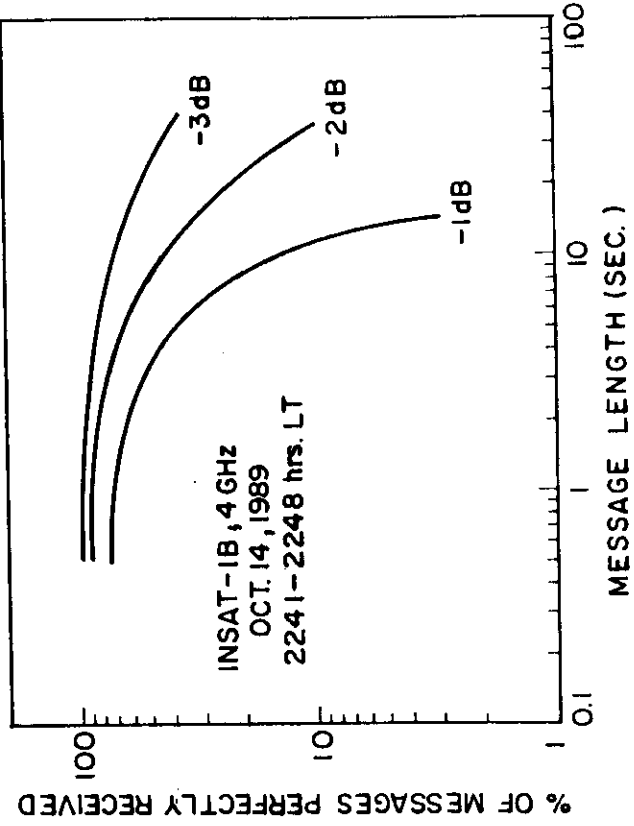


FIGURE 7b

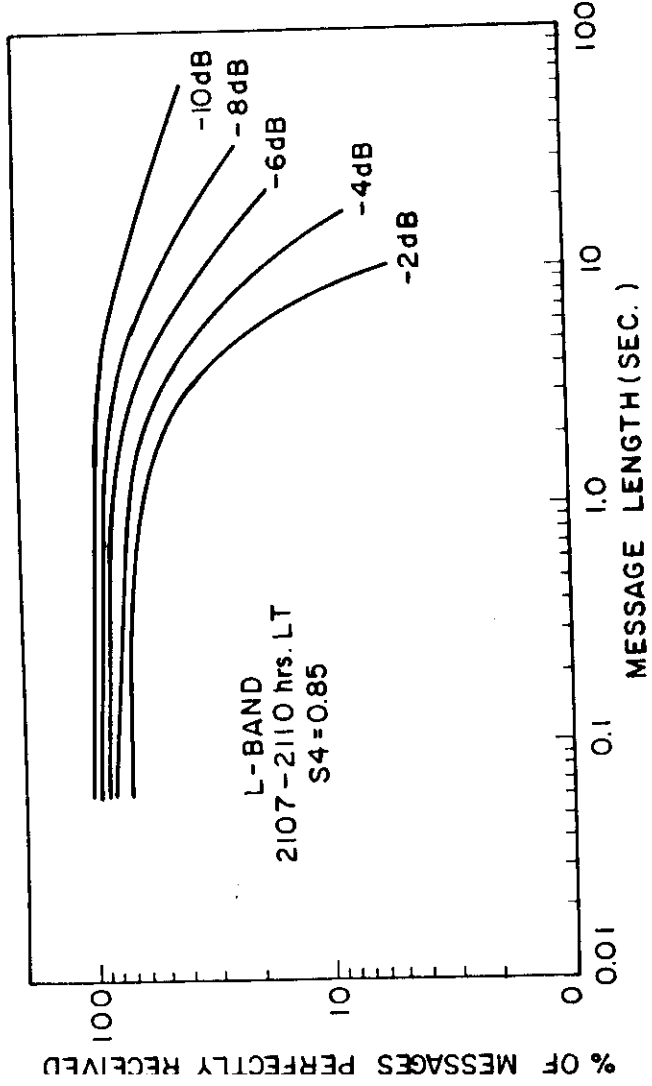


FIGURE 7c

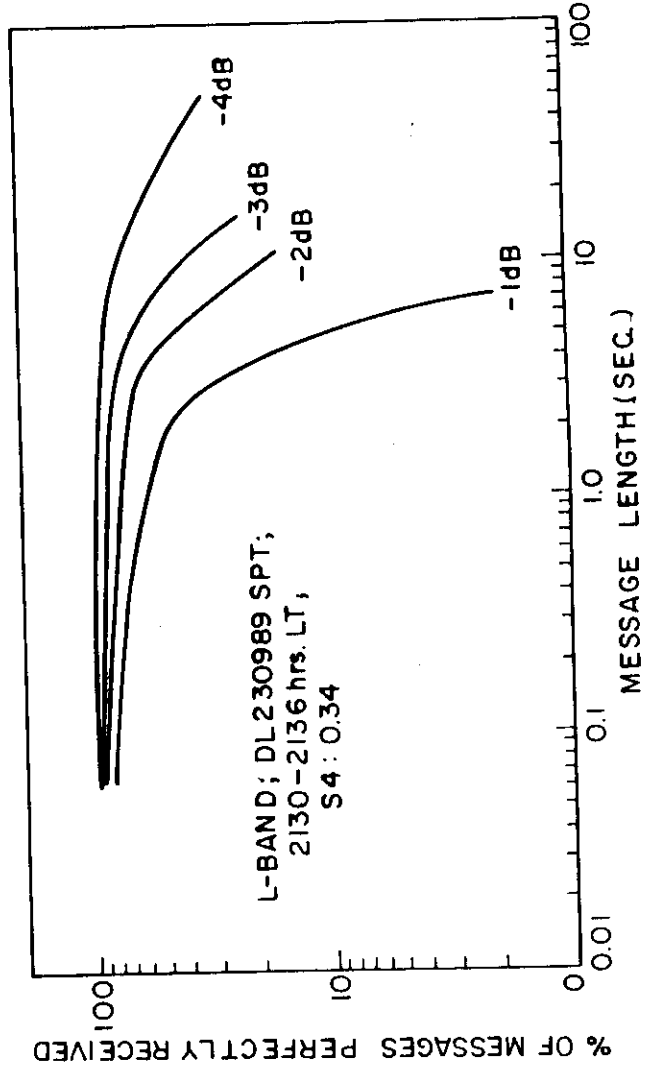


FIGURE 7d

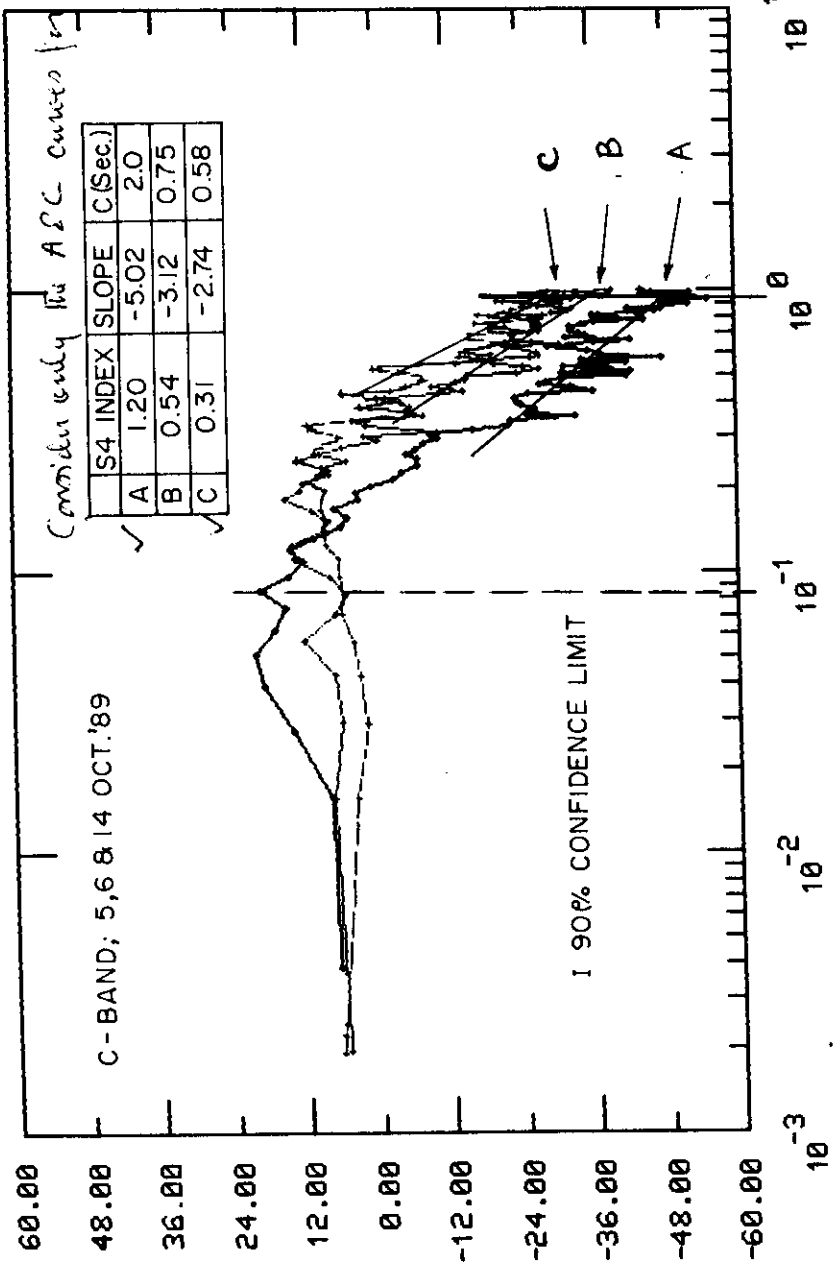


FIGURE 8a

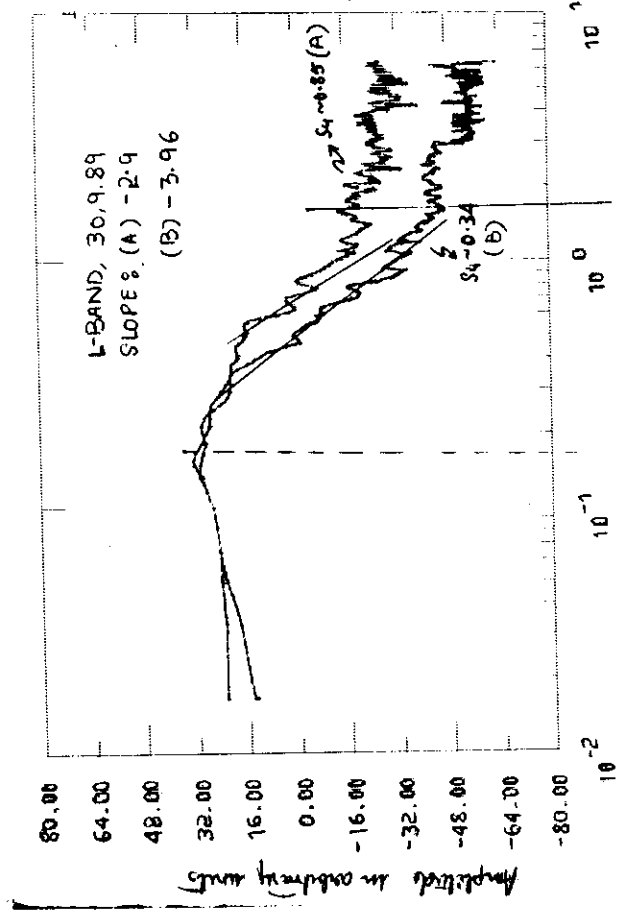


FIGURE 8b

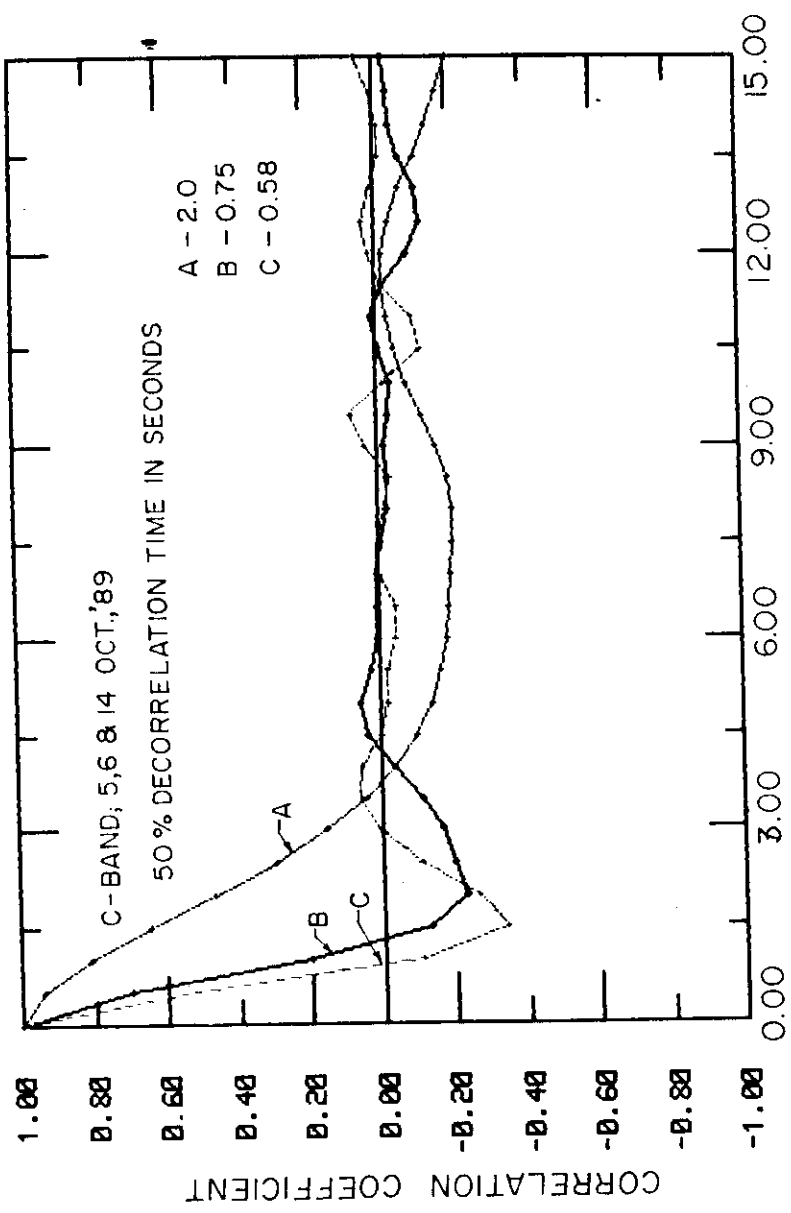


FIGURE 8 90a

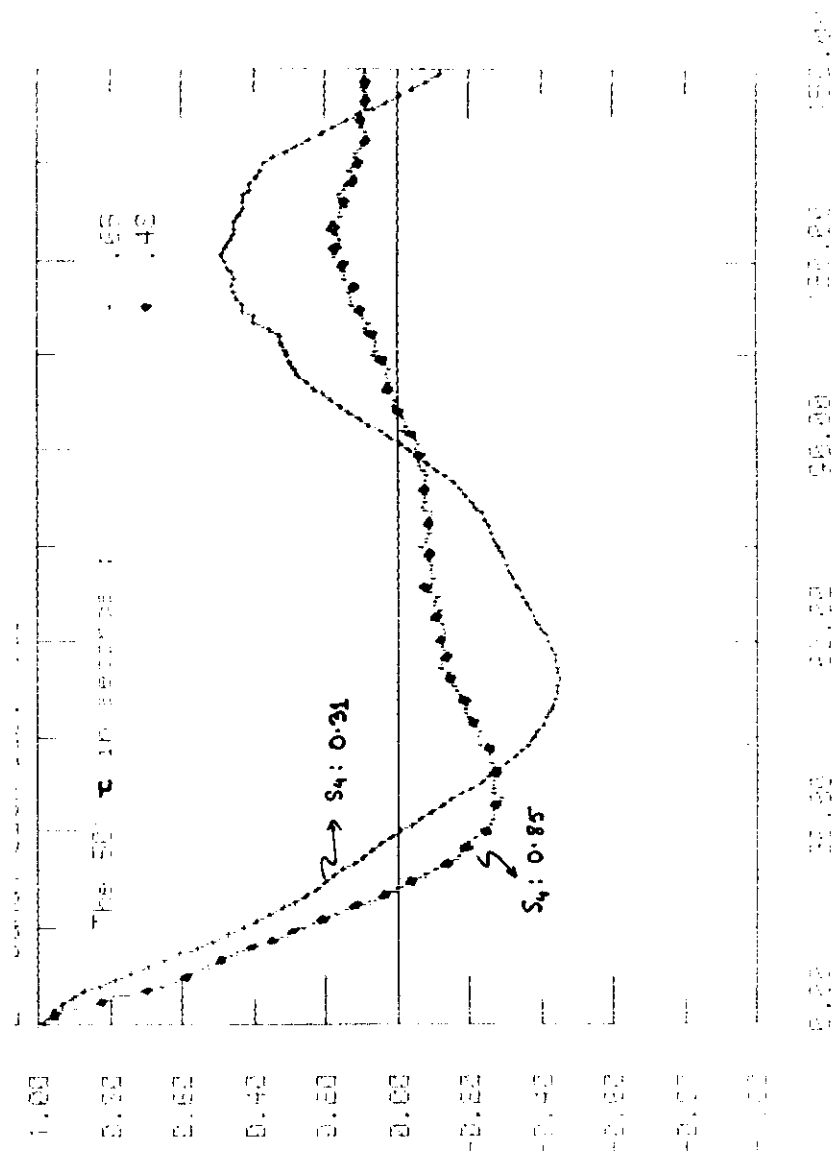


FIGURE 8 90b

